

# The effect of Compton drag on the dynamics of dissipative Poynting dominated flows: Implications for the unification of radio loud AGN

A. Levinson,<sup>1\*</sup> N. Globus,<sup>2</sup>

<sup>1</sup>*Raymond and Beverly Sackler School of Physics & Astronomy, Tel Aviv University, Tel Aviv 69978, Israel*

<sup>2</sup>*Racah Institute of Physics, The Hebrew University of Jerusalem, 91904 Jerusalem, Israel*

Released 18 January 2016

## ABSTRACT

The dynamics of a dissipative Poynting dominated flow subject to a radiation drag due to Compton scattering of ambient photons by relativistic electrons accelerated in reconnecting current sheets is studied. It is found that the efficiency at which magnetic energy is converted to radiation is limited to a maximum value of  $\epsilon_c = 3l_{dis}\sigma_0/4(\sigma_0 + 1)$ , where  $\sigma_0$  is the initial magnetization of the flow and  $l_{dis} \leq 1$  the fraction of initial Poynting flux that can dissipate. The asymptotic Lorentz factor satisfies  $\Gamma_\infty \geq \Gamma_0(1 + l_{dis}\sigma_0/4)$ , where  $\Gamma_0$  is the initial Lorentz factor. This limit is approached in cases where the cooling time is shorter than the local dissipation time. A somewhat smaller radiative efficiency is expected if radiative losses are dominated by synchrotron and SSC emissions. It is suggested that under certain conditions magnetic field dissipation may occur in two distinct phases: On small scales, asymmetric magnetic fields that are advected into the polar region and dragged out by the outflow dissipate to a more stable configuration. The dissipated energy is released predominantly as gamma rays. On much larger scales, the outflow encounters a flat density profile medium and re-collimates. This leads to further dissipation and wobbling of the jet head by the kink instability, as found recently in 3D MHD simulations. Within the framework of a model proposed recently to explain the dichotomy of radio loud AGN, this scenario can account for the unification of gamma-ray blazars with FRI and FRII radio sources.

**Key words:** . galaxies: active - quasars: general - radiation mechanism: nonthermal - gamma-rays: galaxies - galaxies: jets

## 1 INTRODUCTION

A key issue in the theory of magnetized outflows is the dissipation of magnetic energy. A plausible dissipation mechanism commonly invoked is magnetic reconnection (Romanova & Lovelace 1992, Levinson & van Putten 1997, Drenkhahn & Spruit 2002 (DS02); Lyutikov & Blandford 2003; Giannios & Spruit 2007; Lyubarsky 2010; McKinney & Uzdensky 2012, Levinson & Begelman 2013, Bromberg & Tchekhovskoy 2015). This mechanism requires formation of small scale magnetic domains with oppositely oriented magnetic field lines. Such structures may inherently form during outflow injection, as in the striped wind model, or result from current-driven instabilities induced during the propagation of the jet (Mignone et al. 2010, Mizuno et al. 2012, O’Neill et al. 2012, Guan et al. 2014, Bromberg & Tchekhovskoy 2015).

DS02 constructed a model for a dissipative Poynting-flux dominated outflow in GRBs, assuming that magnetic reconnection proceeds at a rate governed by the Alfvén speed, and allowing for isotropic emission in the outflow rest frame. They have shown that

the release of magnetic energy gives rise to effective acceleration of the jet even in the presence of strong radiative losses. In the optimal case, the efficiency at which Poynting energy is converted to nonthermal radiation can approach 50%. The remaining Poynting energy is converted to bulk kinetic energy. This upper limit on the radiative efficiency is a consequence of the kinematic conditions. It can be achieved provided that nearly all the Poynting energy dissipates above the photosphere, on scales at which the cooling rate exceeds the local dissipation rate.

In certain circumstances the flow may be subject to a strong radiation drag (Phinney 1987, Li et al. 1992, Sikora et al. 1996, Beskin et al. 2004, Levinson 2007, Golan & Levinson 2015). This may be the case, e.g., in powerful AGN and in microquasars. The loss of bulk momentum by radiative friction should lead to reduced acceleration of the Poynting dominated flow and a higher radiative efficiency that can exceed the limit found in DS02. In this paper we extend the model outlined in DS02 to flows propagating in an ambient radiation field, by incorporating source terms that account for scattering of external photons by electrons accelerated in reconnecting current sheets. We solve the dynamical equations numerically and compare the numerical solutions with an analytic solution

\* E-mail: Levinson@wise.tau.ac.il

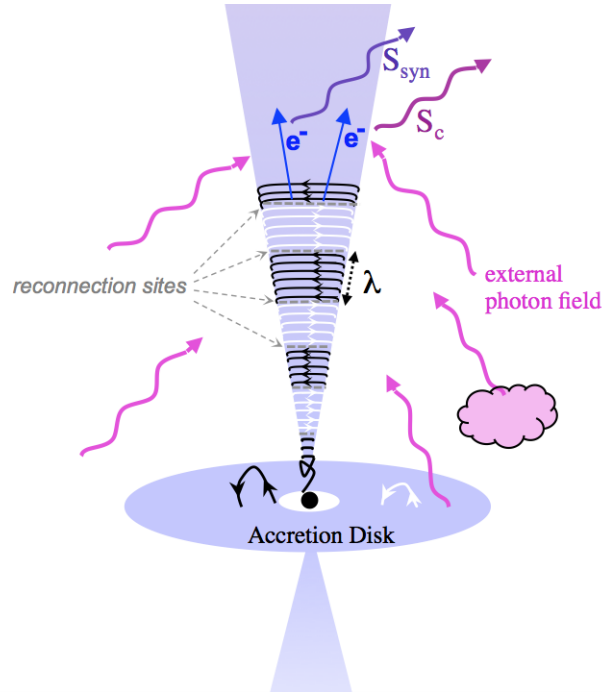


**Figure 1.** Schematic illustration of the outflow model: Advection of asymmetric magnetic field into the black hole gives rise to formation of magnetic domains in the outflow across which the magnetic field changes polarity (indicated by the black and white stripes). Collisionless reconnection in the current sheets separating those domains leads to acceleration of electrons to nonthermal energies. Rapid cooling of the accelerated electrons, via synchrotron emission and inverse Compton scattering of external seed photons, gives rise to effective conversion of the dissipated energy into gamma radiation.

obtained in the limit of rapid cooling. We also derive analytic expressions for the maximum radiative efficiency, and the asymptotic bulk Lorentz factor and magnetization of the outflow.

It has been proposed recently (Tchekhovskoy & Bromberg, 2015) that re-collimation of Poynting dominated jets by ambient gas on kpc scales may explain the FRI- FRII dichotomy of radio loud AGN. In this model, objects having a moderate jet power are significantly slowed down by the ambient medium and appear as FRI sources, owing to a rapid growth of the kink instability, whereas objects having powerful jets are less susceptible to the instability and, therefore, keep propagating at relativistic speeds, forming strong shocks and backflows near the jet head, as seen in FRII sources. However, this scenario ignores the fact that a considerable fraction of the bulk energy must dissipate already on much smaller scales. According to the unified model of radio loud AGN, FRI and FRII sources are associated with blazars when observed at small viewing angles to the jet axis. The strong, highly variable gamma-ray emission observed in many blazars seem to imply high conversion efficiency of Poynting flux to gamma-ray emission on subparsec and parsec scales. If dissipation on those scales is due to internal kink instability, e.g., owing to collimation by disk winds, then one naively expects that by the time the jet reaches kpc scales it will become weakly magnetized, unless fine tuning of external conditions is invoked. Below we propose that dissipation of magnetic energy might naturally occur in two stages, if an unstable magnetic field configuration is established during the injection of the jet. This is expected in cases where the magnetic field advected inwards by the accretion flow has substantial asymmetries. The unstable magnetic field configuration in the jet would then tend to relax to a more stable configuration over scales of the order of the characteristic size of striped layers, typically hundreds of gravitational radii, thereby giving rise to the beamed emission observed

in blazars. Our analysis indicates high radiative efficiency on these scales. It also shows that after relaxing to its stable state, the jet can remain magnetically dominated. Thus, when encountering the confining medium on kpc scales, it can follow the evolution predicted in Tchekhovskoy & Bromberg (2015).

## 2 THE MODEL

We adopt the wind model of DS02, in which magnetic energy is dissipated locally through reconnection during the propagation of the flow (figure 1). Reconnection commences at some radius  $r_0$  at which the 4-velocity of the flow equals  $u_0$ , following an initial acceleration phase in the ideal MHD limit. Local dissipation occurs over a time scale  $\tau = (\lambda/c)\Gamma^2\epsilon^{-1}\sqrt{1+u_A^2}$ , where  $\lambda$  is the characteristic size of the reconnection layer (that is, the distance between neighboring stripes of different magnetic field orientation),  $\Gamma = \sqrt{1+u^2}$  is the bulk Lorentz factor of the flow,  $u_A$  is the local Alfvén 4-velocity in the comoving frame, and  $\epsilon < 1$  is the ratio of the reconnection and Alfvén speeds, with  $\epsilon \approx 0.1$  indicated by recent numerical simulations of relativistic reconnection. The scale  $\lambda$  depends on the magnetic structure of the accretion flow, and is poorly constrained. For illustration we adopt  $\lambda = M$ , where  $M$  is the geometric mass of the black hole. As explained in DS02, the fraction of the initial Poynting flux that can dissipate depends on the magnetic field configuration. Various estimates of the magnetization in the emission zones of blazars, as well as energy considerations, seem to suggest that this fraction must be substantial. Here we suppose that dissipation ceases sharply when the magnetization drops below some critical value  $\sigma_c$ . The evolution of the magnetic field is then governed by the equation

$$\partial_r \ln(rbu) = -\frac{\theta(1 - \sigma_c/\sigma)}{c\tau\beta} = -\frac{1}{\beta\delta_B} \left(\frac{\Gamma_0}{\Gamma}\right)^2 \frac{\theta(1 - \sigma_c/\sigma)}{\sqrt{1 + u_A^2}}, \quad (1)$$

where  $\theta(z)$  is a step function, and we define the fiducial length scale

$$\delta_B = \lambda\Gamma_0^2\epsilon^{-1} \gtrsim 10^{17} M_9(\epsilon/0.1)^{-1} (\Gamma_0/10)^2 \text{ cm}. \quad (2)$$

In regions of high magnetization  $u_A \gg 1$ , and we shall henceforth approximate  $\sqrt{1 + u_A^2} = 1$ . With these approximations, the equations governing the dissipative flow are:

$$\frac{1}{r^2} \partial_r [r^2(w' + b^2)\Gamma u] = S^0, \quad (3)$$

$$\frac{1}{r^2} \partial_r [r^2(w' + b^2)u^2 + r^2 b^2/2] + \partial_r p' = S^r, \quad (4)$$

$$\partial_r \ln(rbu) = -\frac{1}{\beta\delta_B} \left(\frac{\Gamma_0}{\Gamma}\right)^2 \theta(1 - \sigma_c/\sigma), \quad (5)$$

$$\partial_r (r^2 \rho' u) = 0. \quad (6)$$

Here  $w' = \rho' + p' + e'$  is the proper specific enthalpy,  $p'$  the pressure,  $\rho'$  the proper density,  $e'$  the internal energy density,  $b = B'/\sqrt{4\pi}$  the normalized, proper magnetic field,  $\Gamma$  is the bulk Lorentz factor and  $u = \Gamma\beta$  the 4-velocity. The source terms  $S^0$  and  $S^r$  account for energy and momentum losses, respectively. In what follows we adopt a relativistic equation of state, whereby  $e' = 3p'$ . The integral of Equation (6) gives the conserved mass flux,

$$\dot{M} = r^2 \rho' u. \quad (7)$$

The total outflow power and Poynting power are given, respectively, by

$$L_j(r) = r^2(w' + b^2)\Gamma u, \quad (8)$$

$$L_b = r^2 b^2 \Gamma u. \quad (9)$$

A fraction of the magnetic energy dissipated in the reconnection layer is tapped for acceleration of electrons to nonthermal energies. Numerical simulations of collisionless magnetic reconnection in electron-positron plasma (Cerutti et al. 2012, Sironi & Spitkovsky 2014, Werner et al. 2014, Kagan et al. 2015) indicate a power law energy distribution,  $dn'_e/d\gamma = \kappa_e \gamma^{-q}$ ;  $\gamma_1 < \gamma < \gamma_2$ , with index  $q$  that depends on the magnetization parameter of the flow outside the current sheet,  $\sigma = b^2/(\rho' c^2)$ . For  $\sigma \gtrsim 10$  the spectral index lies in the range  $1 < q < 2$ . Electron acceleration to nonthermal energies is expected also in case of reconnection in electron-proton plasma (Melzani et al. 2014, Sironi et al. 2015). Henceforth, we employ the parametrization  $\xi_e = u'_e/e'$ , where  $u'_e = \int m_e c^2 \gamma dn'_e$  is the total energy density of the nonthermal population, as measured in the comoving frame. If equipartition between electrons and protons is established, as seems to be indicated by recent PIC simulations of reconnection in electron-proton plasma (Melzani et al. 2014, Sironi et al. 2015), then  $\xi_e \approx 0.5$ . For a flat distribution,  $q < 2$ , the maximum energy of accelerated electrons,  $\gamma_2$ , is limited by the energy budget. Specifically, for an electron-proton plasma in rough equipartition it is given by  $\gamma_2 \approx (m_p/2m_e)\sigma$  if  $q \approx 1$ , and may be considerably higher for a steeper distribution (Melzani et al. 2014), with  $\gamma_2 \sim (m_p/m_e)[(\sigma + 1)(2 - q)/(2q - 2)]^{1/(2-q)}$  for  $1 < q \lesssim 2$ . Thus, for  $\sigma > \text{a few}$ , we anticipate  $\gamma_2 \gtrsim 10^5$  in electron-proton plasma, consistent with observations of gamma-ray blazars.

Compton scattering of ambient photons by the nonthermal electrons accelerated in reconnection sites imposes a drag force on the flow. We denote the total energy density of the external radiation field by  $u_s(r) = u_{s0} f_s(x)$ , where  $x = r/\delta_B$ . To order  $O(\Gamma^{-2})$  the

source terms associated with the Compton drag are given by (Golan & Levinson 2015)

$$S_c^0 = -\frac{8}{3}\Gamma^3 <\gamma^2> u_s \sigma_T n'_e, \quad (10)$$

$$S_c^r = \beta S_c^0 + S_c^0/3\Gamma^2, \quad (11)$$

in terms of the total electron density

$$n'_e = \int_{\gamma_1}^{\gamma_2} \frac{dn'_e}{d\gamma} d\gamma, \quad (12)$$

and the second moment

$$<\gamma^2> = \frac{1}{n'_e} \int_{\gamma_1}^{\gamma_2} \gamma^2 \frac{dn'_e}{d\gamma} d\gamma. \quad (13)$$

The first and second moments of the electron energy distribution are related to the maximum energy via  $<\gamma^2> / <\gamma> = \chi \gamma_2$ , here

$$\chi = \frac{(2-q)[1 - (\gamma_2/\gamma_1)^{3-q}]\gamma_1}{(3-q)[1 - (\gamma_2/\gamma_1)^{2-q}]\gamma_2}. \quad (14)$$

For the flat spectra observed in simulations of relativistic reconnection we estimate  $\chi \approx (2-q)/(3-q)$ . Using the above parametrization, the energy source term associated with inverse Compton emission can be written as

$$S_c^0 = -\frac{\alpha f_s(x)(\Gamma/\Gamma_0)e}{\delta_B}, \quad (15)$$

in terms of the internal energy density  $e = \Gamma^2 e'$ , and the dimensionless parameter

$$\begin{aligned} \alpha &= \frac{8\delta_B \sigma_T \chi \xi_e \Gamma_0 \gamma_2 u_{s0}}{3m_e c^2} \\ &= 32\chi \xi_e \left(\frac{l_B}{10^{17} \text{ cm}}\right) \left(\frac{\gamma_2}{10^5}\right) \left(\frac{\Gamma_0}{10}\right) \left(\frac{u_{s0}}{10^{-3} \text{ erg cm}^{-3}}\right). \end{aligned} \quad (16)$$

Note that  $\alpha$  is roughly the ratio of the dissipation time at the initial radius  $r_0$ ,  $\tau_0 = \delta_B/c$ , and the cooling time  $t_c = 3m_e c/(4\Gamma_0 \gamma_2 \sigma_T u_{s0})$ . Specifically  $\alpha = 2\chi \xi_e \tau_0/t_c$ . As explained above, in general  $\gamma_2$  depends on the local magnetization  $\sigma$ . However, as will be shown below, in the regime  $\alpha f_s(x) > 1$  the solution is highly insensitive to the value of  $\alpha$ , and we shall henceforth assume, for simplicity, that  $\gamma_2$  is constant.

Synchrotron radiation also contributes to energy losses. We denote by  $S_{\text{syn}}^0$  the source term associated with synchrotron losses. Since the emission is isotropic in the rest frame of the flow one readily obtains  $S_{\text{syn}}^r = \beta S_{\text{syn}}^0$ . The total losses are given by  $S^0 = S_c^0 + S_{\text{syn}}^0$ ,  $S^r = \beta S^0 + S_c^0/3\Gamma^2 = \beta S^0 + \xi_e S^0/3\Gamma^2$ , where we define  $\xi_c = S_c^0/S^0$ .

Equations (3)-(6) can be rendered dimensionless upon using the normalization  $l_j(r) = L_j(r)/L_{j0}$ ,  $l_b(r) = L_b(r)/L_{b0}$ ,  $\bar{\Gamma}(r) = \Gamma/\Gamma_0$ , where subscript 0 denotes values at  $r = r_0$ , and defining the constant fractions  $\kappa_B = L_{b0}/L_{j0}$ , and  $\kappa_w = Mc^2\Gamma_0/L_{j0}$ . In terms of the dimensionless coordinate  $x = r/\delta_B$  one then obtains

$$\frac{dl_j}{dx} = -\frac{3}{4\xi_c} \alpha \bar{\Gamma} f_s(x) (l_j - \kappa_B l_b - \kappa_w \bar{\Gamma}), \quad (17)$$

$$\frac{d \ln \bar{\Gamma}}{dx} = \frac{(4\xi_c/3 - 1) \frac{dl_j}{dx} - \kappa_B \frac{dl_b}{dx} + \frac{2}{x} (l_j - \kappa_B l_b - \kappa_w \bar{\Gamma})}{\kappa_w \bar{\Gamma} + 2l_j - 2\kappa_B l_b}, \quad (18)$$

$$\frac{dl_b}{dx} = -\frac{2l_b}{\bar{\Gamma}^2} \theta(1 - \sigma_c/\sigma), \quad (19)$$

subject to the initial conditions  $l_j(x_0) = l_b(x_0) = \bar{\Gamma}(x_0) = 1$ . In deriving Equation (19) we invoked the approximation  $L_b = r^2 b^2 u^2$  that holds in the relativistic limit.

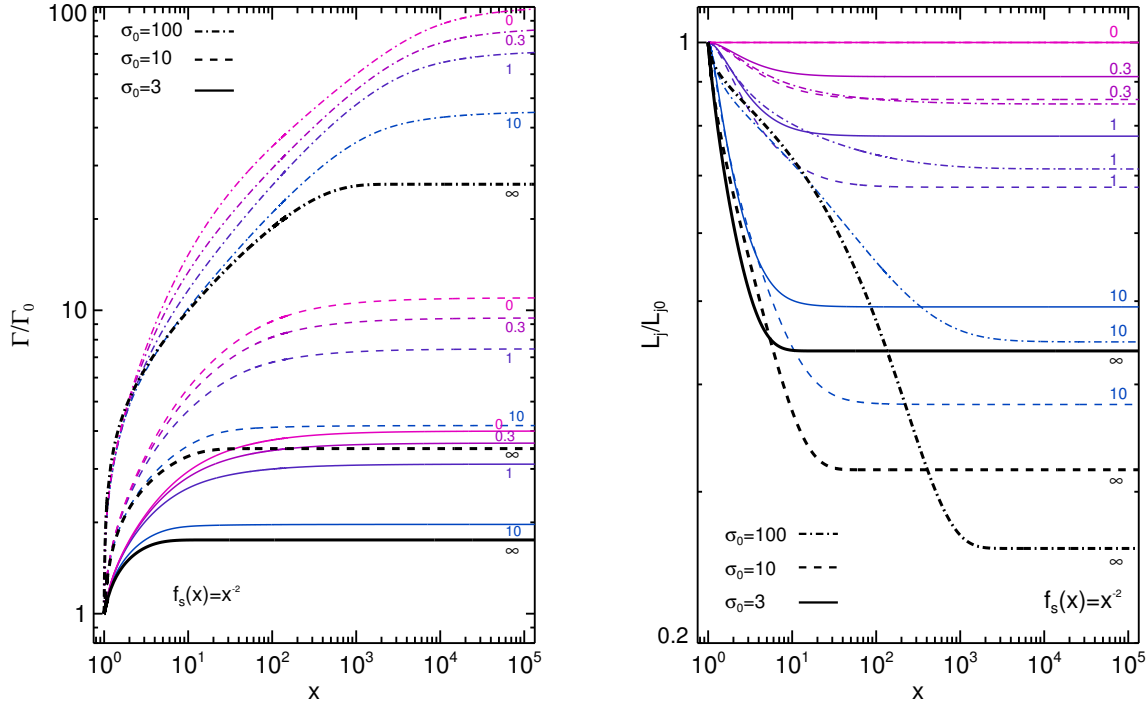


**Figure 2.** Profiles of the normalized Lorentz factor (left) and total jet power (right), computed numerically using Equations (17)-(19) for ambient radiation intensity profile  $f_s(x) = x^{-2}$ , and different values of  $\alpha$  and the initial magnetization  $\sigma_0$ . Different line types correspond to different values of  $\sigma_0$ , as indicated. The numbers that label the curves are the values of  $\alpha$ . The thick black lines delineate the analytic solution, Equations (20)-(22).

### 3 RESULTS

We integrate Equations (17)-(19), starting at  $x = 1$  ( $r = r_0 = \delta_B$ ), where  $\Gamma = \Gamma_0$  and  $l_j = l_b = 1$ . The plasma is assumed to be cold at the injection point, in which case  $\kappa_B = 1 - \kappa_w = \sigma_0/(1 + \sigma_0)$ , where  $\sigma_0 = \kappa_B/\kappa_w$  is the initial magnetization. We consider first the limit where energy losses are dominated by Compton scattering of external radiation, and set  $\xi_c = 1$ . We examine two models for the intensity profile of the external radiation which is intercepted by the flow. In the first one it scales like that of a point source,  $f_s(x) = x^{-2}$ . In the second one  $f_s(x) = 1$  at  $1 < x < x_e$  and  $f(x) = (x/x_e)^{-2}$  at  $x > x_e$ . The latter choice is motivated by detailed calculations of the seed photon field contributed by extended radiation sources in blazars (Joshi et al. 2014).

When  $\alpha \gg 1$  the cooling time is much shorter than the dissipation time of magnetic energy. Then, the dissipated energy is radiated away instantaneously, keeping the internal energy small,  $e' \ll p'$ , so that  $L_j \approx L_b + Mc^2\Gamma$ . To order  $O(\alpha^{-1})$  Equations (17) and (18) admit the analytic solution

$$l_j = 1 - \frac{3\sigma_0}{4(\sigma_0 + 1)}(1 - l_b), \quad (20)$$

$$\bar{\Gamma} = 1 + \frac{\sigma_0}{4}(1 - l_b). \quad (21)$$

Substituting Equation (21) into Equation (19) we obtain the Poynting flux profile:

$$-\left(\frac{\sigma_0}{4} + 1\right)^2 \ln l_b - \frac{\sigma_0}{8}(\sigma_0 + 4)(1 - l_b) + \frac{\sigma_0^2}{32}(1 - l_b^2) = 2(x - 1) \quad (22)$$

at  $x < x_{bc}$  and  $l = l_{bc}$  at  $x > x_{bc}$ , where  $l_{bc} = l_b(x = x_{bc})$  denotes the fraction of the Poynting flux that cannot dissipate. It is related to the critical magnetization  $\sigma_c$  through  $l_{bc} = (1 + 4/\sigma_0)/(1 + 4/\sigma_c)$ . It

is readily seen that in general the asymptotic power, Lorentz factor and magnetization assume the bounds

$$l_{j\infty} \geq 1 - \frac{3\sigma_0}{4(\sigma_0 + 1)}(1 - l_{bc}), \quad (23)$$

$$\Gamma_{\infty}/\Gamma_0 \geq 1 + \frac{\sigma_0}{4}(1 - l_{bc}), \quad (24)$$

$$\sigma_{\infty} = \sigma_0 l_{bc}/\bar{\Gamma}_{\infty} \leq \frac{4\sigma_0 l_{bc}}{4 + \sigma_0(1 - l_{bc})}. \quad (25)$$

In the case of complete dissipation,  $l_{bc} = 0$ , the latter reduce to

$$l_{j\infty} \geq \frac{\sigma_0 + 4}{4(\sigma_0 + 1)}, \quad (26)$$

$$\Gamma_{\infty} \geq \Gamma_0(1 + \sigma_0/4). \quad (27)$$

Evidently, the asymptotic power lies in the range  $1 \geq l_{j\infty} \geq 0.25$  for  $0 \leq \sigma_0 \leq \infty$ . The radiative efficiency is limited to  $\epsilon_c = 3\sigma_0/4(\sigma_0 + 1) \rightarrow 0.75$  at  $\sigma_0 \rightarrow \infty$ . This limit can be approached in highly magnetized flows provided  $\alpha f_s(x)$  remains large on scales over which complete dissipation of the magnetic field occurs. It is worth noting that the above analysis ignores Compton scattering off cold electrons in the flow, which is negligible in the systems under consideration.

Numerical solutions of Equations (17)-(19) are exhibited in figures 2 and 3, for models 1 and 2 respectively. The right panels delineate the evolution of the normalized total power  $l_j$ , and the left panels the evolution of the Lorentz factor  $\Gamma/\Gamma_0$ . Each group of lines of a given type correspond to solutions with the same initial magnetization  $\sigma_0$  and different values of  $\alpha$ , as indicated. The thick black lines correspond to the analytic solution given by Equations (20)-(22). As seen, this solution is a good approximation in the regime  $\alpha f_s(x) > 1$ . We find that even for  $\alpha < 1$  substantial losses

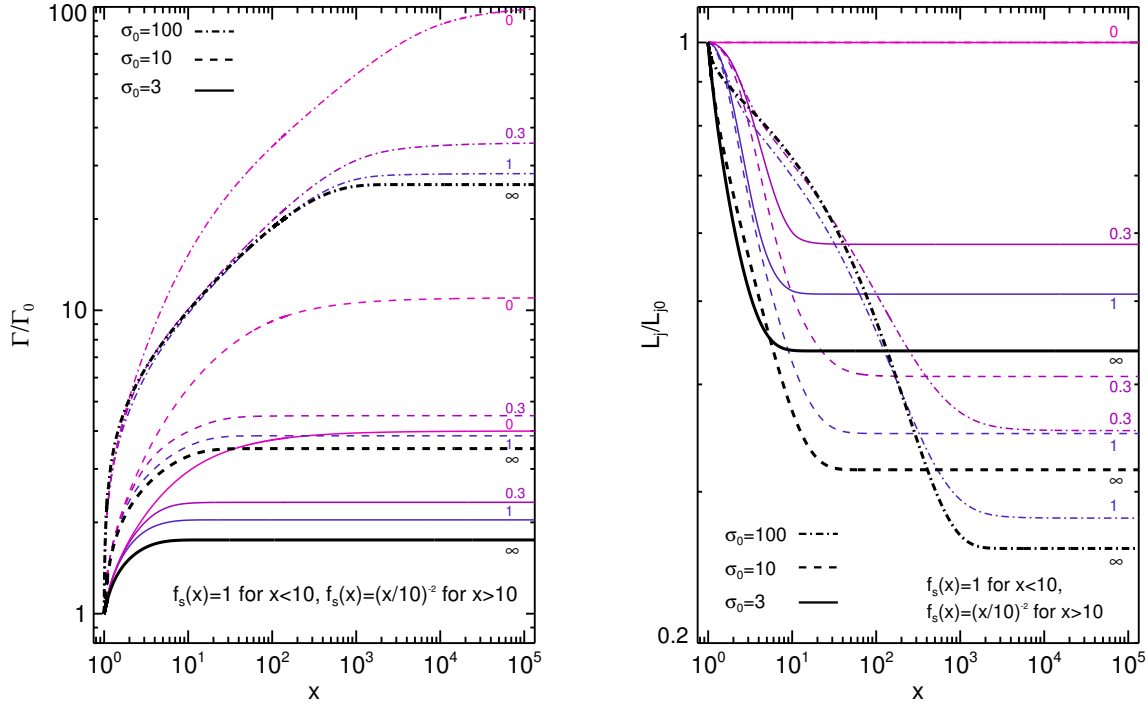


**Figure 3.** Same as figure 2, but for ambient radiation intensity profile  $f_s(x) = 1$  for  $x < 10$  and  $f_s(x) = x^{-2}$  for  $x \geq 10$ .

are expected. For example, for  $\alpha = 0.3$  in figure 3 the radiative losses exceed 50% for flows with  $\sigma_0 \gg 1$ .

In cases where radiative losses are dominated by synchrotron and SSC emission, for which  $\xi_c = 0$ , we recover the result

$$l_j = 1 - \frac{\sigma_0}{2(\sigma_0 + 1)}(1 - l_b), \quad (28)$$

$$\bar{\Gamma} = 1 + \frac{\sigma_0}{2}(1 - l_b), \quad (29)$$

obtained in DS02 in the case of strong radiative losses. For complete dissipation,  $l_{bc} = 0$ , the asymptotic values approach  $l_{j\infty} \rightarrow 0.5$  and  $\Gamma \rightarrow \Gamma_0(1 + \sigma_0/2)$  in the limit  $\sigma_0 \gg 1$ .

#### 4 DISCUSSION

Dissipative Poynting-flux dominated flows can be very efficient emitters of electromagnetic radiation. In sources whereby the plasma in the reconnection zone cools predominantly through inverse Compton scattering of ambient radiation, up to 75% of the initial outflow power can be converted to gamma rays, provided that nearly complete dissipation of the magnetic field occurs, and that in the dissipation region the cooling rate exceeds the local dissipation rate. If the cooling is dominated by synchrotron and SSC emission, the radiative efficiency is lower,  $\epsilon_c \leq 0.5$ .

If dissipation commences at  $\Gamma_0 \sim$  a few, then we anticipate  $\delta_B \approx 10^2 - 10^3 M$  for typical reconnection speeds observed in recent numerical simulations,  $v_r \lesssim 0.1c$ . If the luminosity of the radiation intercepted by the jet is a fraction  $\eta$  of the Eddington value, then we estimate  $\alpha \approx 3 \times 10^{10} \eta (r_g/\delta_B)^2 \gtrsim 10^4 \eta$ , independent of the mass of the central engine. Thus, we anticipate radiative friction to be important in luminous, Galactic and extragalactic sources. Detailed calculations (Joshi et al 2014) show that in a prototypical blazar,

like 3C279, the energy density of radiation intercepted by the jet is roughly constant,  $u_s \approx 10^{-3}$  ergs cm $^{-3}$ , inside the broad line region, up to a radius of  $r \approx 10^{18}$  cm, and then declines roughly as  $r^{-2}$ . This profile corresponds to our model 2 shown in figure 3. Taking  $\xi_e = 0.5$  and a power law index  $q = 1.5$  for which  $\chi = 0.3$ , we estimate  $\alpha \gtrsim 4$  from Equation (16). From figure 3 we expect high radiative efficiency in those objects, as indeed inferred from observations. In the TeV blazars, synchrotron and SSC emission most likely dominate. The radiative efficiency is then lower, but can still approach 25% even if only half of the Poynting energy dissipates in the TeV emission zone.

An interesting possibility is that complete magnetic field dissipation occurs, under certain conditions, in two distinct stages. On small scales, the unstable magnetic field configuration established during the injection of the outflow relaxes to a more stable configuration. During this stage gamma-ray emission is produced with high efficiency. Nonetheless, the jet remains magnetically dominated if only a fraction of the Poynting flux can dissipate. On vastly larger scales, the outflow encounters a flat density profile medium and re-collimates. If its magnetization remains sufficiently high,  $\sigma \sim$  a few, when reaching those scales, then its subsequent evolution would depend on its relative power, as shown recently in the case of AGN (Tchekhovskoy & Bromberg 2015). Powerful jets will not be affected significantly by the external medium and will propagate stably to large distances at relativistic speeds, forming strong shocks at the jet head. At large viewing angles those appear as FRII radio sources. Less powerful jets are susceptible to the kink instability (Bromberg & Tchekhovskoy 2015), leading to further dissipation of the magnetic energy and wobbling of the jet head that slows it down. Those would appear as FRI radio sources. In both cases we expect strongly beamed gamma-ray emission on sub-parsec and parsec scales, that can be detected in sources observed at

small viewing angles, consistent the unified scheme for radio loud AGNs. For instance, if the initial magnetization is  $\sigma_0 = 50$  and only half of the initial Poynting energy can dissipate during the first stage, then from Equation (23)-(25) we obtain gamma-ray production efficiency of  $1 - l_j \simeq 0.37$ , Lorentz  $\Gamma \simeq 7\Gamma_0$  and magnetization  $\sigma \simeq 3.5$  at the end of the first stage. If radiation drag is insignificant, as might be the case in the fainter sources, the gamma-ray production efficiency may be somewhat smaller, 0.25, as seen from Equation (28), and the Lorentz factor somewhat higher,  $\Gamma \simeq 12\Gamma_0$ . If the flow remains roughly conical during its subsequent evolution, then it will be magnetically dominated when encountering the flat density medium, and the analysis of Tchekhovskoy & Bromberg (2015), as described above, applies.

## ACKNOWLEDGMENTS

We thank Lorenzo Sironi for useful comments.

AL acknowledges the support of The Israel Science Foundation (grant 1277/13). NG acknowledges the support of the I-CORE Program of the Planning and Budgeting Committee, The Israel Science Foundation (grant 1829/12) and the Israel Space Agency (grant 3-10417).

## REFERENCES

- Begelman M. C., 1998, *ApJ*, 493, 291  
Beskin V. S., Zakamska N. L. & Sol H., 2004, *MNRAS*, 347, 587  
Bromberg O. & Tchekhovskoy A., 2015, *arXiv:1508.02721*  
Cerutti B., Uzdensky D. A. & Begelman M. C., 2012, *ApJ*, 746, 148  
Drenkhahn G. & Spruit H. C., 2002, *A&A*, 391, 1141  
Golan O. & Levinson A., 2015, *ApJ*, 809, 23  
Giannios D. & Spruit H. C., 2007, *A&A*, 469, 1  
Guan X., Li H., Li S., 2014, *ApJ*, 781, 48  
Joshi M., Marscher A. P. & Bottcher M., 2014, *ApJ*, 785, 132  
Kagan, D. Sironi, L. Cerutti, B. & Giannios, D., 2015, *SSR*, 191, 545  
Levinson A. & van Putten M. H. P. M., 1997, *ApJ*, 488, 69  
Levinson A. 2007, *ApJ*, 671, L29  
Levinson A. & Begelman, M. C. 2013, *ApJ*, 764, 148  
Li Z., Begelman M. C. & Chiueh T., 1992, *ApJ*, 384, 567  
Lyubarsky Y., 2010, *ApJ*, 725, L234  
Lyutikov M. & Blandford R. D., 2003, preprint (*astro-ph/0312347*)  
McKinney J. C. & Uzdensky D. A., 2012, *MNRAS*, 419, 573  
Melzani M. et al., 2014, *A&A*, 570, 112  
Mignone A., Rossi P., Bodo G., Ferrari A., Massaglia S., 2010, *MNRAS*, 402, 7  
Mizuno Y., Lyubarsky Y., Nishikawa K.-I., Hardee P. E., 2012, *ApJ*, 757, 16  
O’Neill S. M., Beckwith K., Begelman M. C., 2012, *MNRAS*, 422, 1436  
Phinney, E., 1987, in Zensus J. A, Pearson T. J., eds, *Superluminal Radio Sources*. Cambridge Univ. Press, Cambridge, p.301  
Romnanova, M. M. & Lovelace, R. V. E., 1992, *A&A*, 262, 26  
Sikora M., Sol H., Begelman M. C. & Madejski G. M., 1996, *MNRAS*, 280, 781  
Sironi L. & Spitkovsky A. ,2014, *APJ*, 783, L21  
Sironi L., Petropoulou M. & Giannios D., 2015, *arXiv1502.0102*  
Tchekhovskoy A. & Bromberg O., 2015, *arXiv:1512.04526*

Werner G. R., Uzdensky D. A., Cerutti B., Nalewajko K. & Begelman M., 2014 *arXiv:1409.8262*